Three-Dimensional Podocyte-Endothelial Cell Co-cultures: Assembly, Validation, and Application to Drug Testing and Intercellular Signaling Studies

Min Li[a]*, Alessandro Corbelli[a,b], Shojiro Watanabe[a], Silvia Armelloni[a], Masami Ikehata[a], Valentina Parazzi[c], Chiara Pignatari[a], Laura Giardino[a], Deborah Mattinzoli[a], Lorenza Lazzari[c], Aldamaria Puliti[d], Francesco Cellesi[a,e,f], Cristina Zennaro[g], Piergiorgio Messa[a], Maria Pia Rastaldi[a]

[a] Renal Research Laboratory, Fondazione IRCCS Ca' Granda Ospedale Maggiore Policlinico & Fondazione D'Amico per la Ricerca sulle Malattie Renali, via Pace 9, 20122 - Milan, Italy.

[b] Bio-imaging Unit, Department of Cardiovascular Research, IRCCS – Istituto di Ricerche Farmacologiche Mario Negri, via La Masa 19, 20156 - Milan, Italy.

[c] Cell Factory, Unit of Cell Therapy and Cryobiology, Fondazione IRCCS Ca' Granda Ospedale Maggiore Policlinico, via Pace 9, 20122 - Milan, Italy.

[d] Department of Neurosciences, Rehabilitation, Ophthalmology, Genetics, Maternal and Child Health (DiNOGMI), University of Genoa, and Medical Genetics Unit, Istituto Giannina Gaslini, via G. Gaslini 5, 16148 - Genoa, Italy.

[e] Department of Chemistry, Materials, and Chemical Engineering "G.Natta", Politecnico di Milano, via Mancinelli 7, 20131 - Milan, Italy.

[f] Fondazione CEN – European Centre for Nanomedicine, Piazza Leonardo da Vinci 32, 20133 - Milan, Italy.

[g] Laboratory of Renal Physiopathology, Department of Medical, Surgical, and Health Sciences, Trieste University, via Strada di Fiume 447, 34149 - Trieste, Italy.

*Corresponding author: Tel: +39-0255033880; Fax: +39-0255033878; E-mail: li_min@libero.it

E-mail addresses:

LM: li_min@libero.it
CA: alecorbelli@hotmail.com
AS: armellonis@libero.it
WS: swat4028@yahoo.co.jp
GL: giardinolaura@gmail.com
IM: aquamarine0321@libero.it
MD: Deborah.mattinzoli@gmail.com
PV: valentina.parazzi@gmail.com
PC: chiarapignatari@gmail.com
MP: pmessa@policlinico.mi.it
LL: lorenza.lazzari@policlinico.mi.it
ZC: czennaro@units.it
PA: aldamaria.puliti@unige.it
CF: francesco.cellesi@polimi.it
RMP: mariapia.rastaldi@policlinico.mi.it

Abstract

Proteinuria is a common symptom of glomerular diseases and is due to leakage of proteins from the glomerular filtration barrier, a three-layer structure composed by two post-mitotic highly specialized and interdependent cell populations, i.e. glomerular endothelial cells and podocytes, and the basement membrane in between.

Despite enormous progresses made in the last years, pathogenesis of proteinuria remains to be completely uncovered. Studies in the field could largely benefit from an in vitro model of the glomerular filter, but such a system has proved difficult to realize. Here we describe a method to obtain and utilize a three-dimensional podocyte-endothelial co-culture which can be largely adopted by the scientific community because it does not rely on special instruments nor on the synthesis of devoted biomaterials.

The device is composed by a porous membrane coated on both sides with type IV collagen. Adhesion of podocytes on the upper side of the membrane has to be preceded by VEGF-induced maturation of endothelial cells on the lower side.

The co-culture can be assembled with podocyte cell lines as well as with primary podocytes, extending the use to cells derived from transgenic mice.

An albumin permeability assay has been extensively validated and applied as functional readout, enabling rapid drug testing. Additionally, the bottom of the well can be populated with a third cell type, which multiplies the possibilities of analyzing more complex glomerular intercellular signaling events.

In conclusion, the ease of assembly and versatility of use are the major advantages of this three-dimensional model of the glomerular filtration barrier over existing methods. The possibility to run a functional test that reliably measures albumin permeability makes the device a valid companion in several research applications ranging from drug screening to intercellular signaling studies.

Keywords

Glomerular filtration barrier, three-dimensional co-culture, podocytes, endothelial cells, albumin permeability, drug testing, intercellular signaling, mesenchymal stem cells.

1. Introduction

The glomerular filtration barrier is a convoluted capillary formed by a fenestrated endothelium lying on a basement membrane, which is externally covered by specialized cells called podocytes.

Damage to any element of the barrier results in proteinuria, i.e. the leakage of proteins into the urine, a common symptom of glomerular diseases and a major contributor to renal disease progression (Garg and Rabelink, 2011)

Exceptional advances have been reached in recent years, but a full pathophysiological understanding of the mechanisms underlying proteinuric diseases

remains to be achieved and could benefit from a three-dimensional (3D) model of the glomerular filtration barrier allowing functional studies to be conducted in vitro.

Despite the recognized need, co-culturing together in an appropriate fashion the cell components of the glomerular filter has always encountered technical difficulties, most likely due to the peculiar features of glomerular endothelial cells and podocytes, which are both highly differentiated, specialized, and interdependent cell types (Obeidat and Ballermann, 2012; Reiser and Sever, 2013).

As an alternative, several groups have utilized organotypic cultures of renal tissue under continuous perfusion (Avner et al., 1983; Avner et al., 1990; Kloth et al., 1995). With some modification, these methods are still in use, but remain primarily devoted to developmental studies.

In 2002 a sandwich method was described in which primary rat podocytes immortalized by SV-40 transfection were grown on collagen-coated coverslips overlayed with matrigel. Human Umbilical Vein Endothelial Cells (HUVEC) were then seeded on top of the matrigel (Chen et al., 2002; Kim et al., 2002). The main limitation of this model is that podocytes make adhesion to matrix proteins on both their sides and the assembly does not allow to control and maintain a regular distance or even a separation between podocytes and endothelial cells.

In a method subsequently proposed by Hirschberg et al, conditionally immortalized mouse podocytes were grown on cell culture inserts hung into wells. Endothelial cells, derived from circulating precursors, were seeded at the bottom of the wells (Hirschberg et al., 2008). With this procedure, a supernatant separates podocytes and endothelial cells, modifying the spatial relationship between the cell types, the extracellular matrix and the membrane.

More recently, Slater et al realized a co-culture model in which human conditionally immortalized podocytes and glomerular endothelial cells were grown on the opposite

sides of a nanofibre membrane obtained by electrospinning a solution of collagen type I and polycaprolactone on nickel micro-meshes (Slater et al., 2011).

In 2012, Bruggeman et al described the production of thin films of hydrogel suitable for co-culturing podocyte and endothelial cells on the opposite sides of the film (Bruggeman et al., 2012).

To the best of our knowledge, these are the only two models which reproduce a correct relationship between podocytes and endothelial cells. However, both methods were not adopted widely by the scientific community most likely due to the particular requirements for their realization.

Here we propose a 3D co-culture methodology easier to realize than the above systems because it does not need especial instrumentation or expertise in material synthesis. Our results demonstrate that the device can be useful in different applications, and reliable functional information can be obtained by an albumin permeability test. The system can be assembled with primary podocytes, extending the use to transgenic models, and a third cell population can be seeded at the bottom of the well, which enables to get information from more complex intercellular interactions.

2. Materials and Methods

All reagents, when not otherwise specified, were from Sigma-Aldrich (Milan, Italy). Primary, secondary antibodies, and control immunoglobulins are listed in Table 1.

Table 1- Antibodies

Primary antibodies

Name	Company	Dilution
Guinea pig polyclonal anti-nephrin	Progen Cat.No. GP-N2	IF: 1:100
Rabbit polyclonal anti-podocin	Sigma-Aldrich Cat.No. P0372	IF: 1:50
Mouse monoclonal anti-pan cytokeratin	Abcam Cat.No. Ab6401	IF: 1:100
Mouse monoclonal anti-alpha-SMA	Abcam Cat.No. ab7817	IF: 1:200
Rabbit monoclonal anti-CD31	Epitomics Cat.No. 2540-1	IF: 1:200
Mouse monoclonal anti-synaptopodin	Progen Cat.No. 61094	IF: 1:20
Rabbit anti-NMDAR1	Abcam Cat.No. ab17345 (WB)	WB: 1:250
Rabbit anti-NMDAR1	Abcam Cat.No ab28669 (IF)	IF: 1:50
Rabbit policlonal anti-Grm1	Novus Cat.No.NB300-123	IF: 1:50
		WB: 1:500
Rabbit polyclonal anti-P44/42 MAPK	Cell signalling Cat.No.9102	ICE: 1:200
Mouse moloclonal anti-phospho-p44/42-MAPK	Cell signalling Cat.No 9106	ICE: 1:400
Mouse monoclonal anti-VE-cadherin	Abcam Cat.No. ab7047	IF: 1:10
		WB: 1:250
Rabbit polyclonal anti-VWF	Abcam Cat.No. ab9378	1:100

IF: Immunofluorescence. WB: Western Blot. ICE: In-cell ELISA.

Control Immunoglobulins

Name	Company	Dilution
rabbit IgG Isotype control	Invitrogen Cat.No. PA5-23090	From 1:50 to 1:500
mouse IgG1 Isotype control	Invitrogen Cat.No.MA5-14453	From 1:20 to 1:400
G. Pig IgG (non immune), purified	Alpha-Diagnostics Cat.No.ABIN286082	1:100

Secondary Antibodies

Name	Company	Dilution
Alexa Fluor 488 goat anti-rabbit IgG	Invitrogen Cat.No.A11070	1:70
Alexa Fluor 546 goat anti-rabbit IgG	Invitrogen Cat.No.A11035	1:70
Alexa Fluor 488 goat anti-mouse IgG highly cross adsorbed	Invitrogen Cat.No.A11029	1:70
Alexa Fluor 546 goat anti-mouse IgG highly cross adsorbed	Invitrogen Cat.No.A11030	1:70
Alexa Fluor 488 Goat Anti-Guinea Pig IgG highly cross-adsorbed	Invitrogen Cat.No.A11073	1:70

2.1. Cultured Podocytes

For primary cultures, kidneys were taken from 7- to 10-d-old rodents, as described previously (Rastaldi et al., 2006). Briefly, glomeruli were isolated by sieving, then

seeded in culture flasks (Corning, Sigma-Aldrich) pre-coated with collagen type IV at 37°C in 5% CO2 atmosphere and covered by DMEM-F12 medium supplemented with 10% FCS, 5 mg/ml transferrin, 10^{-7}M hydrocortisone, 5 ng/ml sodium selenite, 0.12 U/ml insulin, 100 U/ml penicillin, 100 mg/ml streptomycin, 2 mM L-glutamine. After 1 week, first-passage podocytes were separated from glomeruli by an additional sieving through the 36-µm mesh. Second passage podocytes were seeded on flasks and thermanox coverslips (Nunc, VWR Int., Milan, Italy). Cell characterization was performed by morphology and immunofluorescence, using podocyte (nephrin, podocin), epithelial (cytokeratins), smooth muscle (α-smooth muscle actin), and endothelial cell (CD31) markers.

For the conditionally immortalized cell line (Giardino et al., 2009), we followed with minor modifications the procedure originally published by Mundel et al (Mundel et al., 1997). Briefly, glomeruli were isolated from kidneys of adult (10-wk old) transgenic H-2Kb-tsA58 mice by the same procedure as described above and grown first in standard medium at 37°C. Second-passage cells were re-plated and propagated at 33°C in medium (DMEM-F12, supplemented with 10% FBS, 100 U/ml penicillin, 100 mg/ml streptomycin, 2 mM L-glutamine) containing 20 U/ml recombinant mouse γ-IFN. Limiting dilution (10.0, 1.0, and 0.1 cells/vial) of these cells was followed by characterization, and only five clones expressing WT1 and nephrin on more than 90% of cells were selected and propagated. For initiation of differentiation, cells were thermo-shifted to 37°C and maintained in medium (DMEM-F12, supplemented with 10% FBS, 5 mg/ml transferrin, 10^{-7}M hydrocortisone, 5 ng/ml sodium selenite, 0.12 U/ml insulin, 100 U/ml penicillin, 100 mg/ml streptomycin, 2 mM L-glutamine) without γ-IFN.

2.2 Endothelial cells

The EOMA, mouse microvascular endothelial cell line (Obeso et al., 1997) was obtained from ATCC (ATCC number: CRL-2586, LGC Standards S.r.l., Sesto San Giovanni, Milan, Italy). As indicated by the ATCC protocol, cells were grown in DMEM/F12 supplemented with 10% FBS, 100 U/ml penicillin, 100 mg/ml streptomycin, 4 mM L-glutamine.

Cells were characterized by evaluation of endothelial markers (CD31, VE-Cadherin, and vWF), and uptake of Dil-acetylated-LDL (Acetylated Low Density Lipoprotein, labeled with 1,1'-dioctadecyl–3,3,3',3'-tetramethyl-indocarbocyanine perchlorate, from Life Technologies, Monza, Italy) (Fig 1).

2.3. Isolation and culture of Cord Blood derived Mesenchymal Stem Cells (CBMSC)

Human cord blood (CB) was collected in sterile bags containing 29 mL of citrate-phosphate dextrose (CPD) as anticoagulant (Macopharma, Mouvaux, France) from pregnancies undergoing deliveries after receiving informed consent. CB was processed within 14 hours and mesenchymal stem cells (MSC) were isolated and expanded as described (Barilani et al., 2015). For the experiments, CBMSC were cultured in DMEM/F12 including 20% fetal bovine serum (FBS; Gibco, Life Technologies, Monza, Italy) and 4 mM L-glutamine.

At passage 3, CBMSC cultured under these conditions were harvested using TrypLE Select 1X (Gibco) and stained with 5 µg/mL Hoechst 33258 for 1 hour at 37°C in their culture medium. After staining, the cells were washed once with phosphate-buffered saline (PBS; Macopharma, Mouvaux, France) and seeded at a density of 4000 cells/cm^2 in 24-well cell culture plates with their complete medium.

2.4. Three-dimensional co-culture system and assessment of permeability

Different types of 1µm porous membranes (Millicell hanging cell culture inserts, Millipore, Milan, Italy) were tried, namely the Biopore Membrane (made of hydrophilic polytetrafluoroethylene - PTFE), the Isopore™ Membrane (made of polycarbonate), and the Polyethylene Terephthalate (PET) microporous membrane. All membranes were alternatively coated on both sides with collagen type I or type IV.

Endothelial cells were seeded first on one side of the membrane and covered by medium. Once attached, podocytes were seeded on the other side of the membrane. Alternatively, podocytes were seeded first, followed by endothelial cells.

In a subsequent application, VEGF (from 1 to 50ng/ml) was added for 1 to 10 days to endothelial cells before seeding podocytes on the opposite side of the membrane.

Finally the co-culture system was standardized. Briefly, using the Polyethylene Terephthalate (PET) microporous (1µm diameter) membrane coated on both sides with collagen type IV, 1.5 x 10^5 of Endothelial cells were seeded on the lower side of the membrane and exposed to VEGF 5 ng/ml for one week before 65,000 podocytes were seeded on the upper side of the membrane and covered by their own medium.

To assess albumin permeability, cells were carefully washed on both sides with PBS. Then, the upper (podocyte) compartment was filled by DMEM/F-12 and the lower (endothelial) compartment was filled by DMEM/F12 supplemented with 40mg/ml BSA. Medium was taken from the upper compartment at different time points (30min, 1h, 2h, 3h, 5h) and albumin content measured by spectrometry using the DC protein assay kit (Bio-Rad, Milano, Italy).

Results can be alternatively expressed as absolute values (mg/ml) or as percentages (% BSA permeability versus control conditions).

Coomassie-stained gels were used to confirm that BSA was the only protein present in the medium, excluding the contribution from cellular proteins.

2.5. Renal tissue

Kidneys were obtained from 3 month old C57BL/6 mice. For immunofluorescence, the unfixed renal tissue was embedded in OCT (Tissue-Tek, Electron Microscopy Sciences, SIC, Rome, Italy), snap-frozen in a mixture of isopentane and dry ice, and stored at –80°C until use.

2.6. Immunofluorescence studies

Apart from F-actin, directly detected on paraformaldehyde (PFA)-fixed slides by Phalloidin–TRITC, an indirect immunofluorescence method was applied on 5µm-thick acetone-fixed tissue cryosections and on acetone-fixed cultured cells.

Briefly, after washing, slides were sequentially incubated with the primary antibody, followed by the appropriate fluorescent-labelled secondary antibody. Specificity of Ab labelling was demonstrated by the lack of staining after substituting control immunoglobulins for the primary antibodies.

Slides were mounted with Fluorsave aqueous mounting medium (Merck, Milano, Italy).

Images were acquired by Zeiss Axioscope 40FL microscope, equipped with AxioCam MRc5 digital videocamera and immunofluorescence apparatus (Carl Zeiss SpA), and recorded by AxioVision software 4.3, or by Zeiss AxioObserver microscope equipped with high resolution digital videocamera (AxioCam, Zeiss) and Apotome system for structured illumination, and recorded by AxioVision software 4.8.

2.7. Western Blot

As previously described (Giardino et al., 2009), cells were lysed in RIPA buffer, protein lysates were separated on a SDS-PAGE and transferred by electroblotting on a PVDF membrane (ImmunBlot PVDF membrane, BioRad Laboratories Inc., CA,

USA). After blocking, each membrane was incubated with the primary antibody, followed by the proper HRP (horseradish peroxidase)-conjugated secondary antibody, and positive reaction products were identified by chemiluminescence (BM Chemiluminescence Western Blotting Kit, Roche, Mannheim, Germany). Negative controls were performed by loading buffer instead of the protein lysate. Images were digitally acquired by Chemidoc XRS instrument (Bio-Rad, Milan, Italy).

2.8. Light and Electron Microscopy

After experiments, membrane insets were carefully removed from their holding apparatus.

For light and transmission electron microscopy, the insets were fixed in a mixture of paraformaldehyde and glutaraldehyde in phosphate buffer 0.12M, post-fixed in osmium tetroxide 1% in cacodylate buffer 0.12M, dehydrated, and embedded in Epon-Araldite resin.

Semithin sections were cut perpendicular to the membrane, stained by toluidine blue, and observed by light microscopy.

Ultra-thin sections were then cut and placed on grids, stained by uranyl-acetate and lead-citrate, and observed under a CM10 Philips microscope (FEI, Eindhoven, The Netherlands).

For scanning electron microscopy, the insets were fixed in a mixture of glutaraldehyde 2% and paraformaldehyde 4% in phosphate buffer 0,12 M for 6 h, fixed in a mixture of osmium tetroxide 1% and sodium cacodylate buffer 0,12M for 2 h, dehydrated in a graded ethanol series and dried in hexamethyldisilazane. Then the pieces were sputter-coated with gold (Edwards S150A sputter coater) and observed under a XL30 Philips microscope. All reagents and grids for electron microscopy were from Electron Microscopy Sciences.

2.9. Immunogold Electron Microscopy

An indirect immunogold labelling procedure was performed on ultrathin kidney sections, as described previously (Giardino et al., 2009). Briefly, after blocking, the material was incubated with the primary antibody followed by a 12nm-gold-conjugated secondary antibody (Jackson ImmunoResearch Europe, Suffolk, UK). Specificity of antibody labelling was demonstrated by the lack of staining after substituting control immunoglobulins for the primary antibody.

2.10. In-Cell ELISA

To get quantification of protein expression data, we used the In-Cell ELISA colorimetric detection kit (Thermo Scientific, Euroclone, Milan, Italy), according to the manufacturer's instructions.

All steps were conducted on the appropriate side of the membrane.

After 4% buffered paraformaldehyde fixation, cells were sequentially incubated with the "Permeabilization Buffer", the "Quenching Solution", and the "Blocking Buffer". The primary antibody was then added, followed by the HRP-conjugated secondary antibody and 3,3',5,5'-Tetramethylbenzidine (TMB) substrate. The reaction was stopped after 15min with the "TMB Stop Solution" and absorbance was immediately measured at 450nm wavelength. After washing, Janus Green Whole-Cell Stain was added for 5 min. Careful washing was followed by addition of "Elution Buffer" and absorbance was read at 615nm. Replicate background measurements were subtracted to all 450nm measures. The resulting A450 values were then normalized to the A615 values to account for differences in cell number.

2.11. Cell proliferation assay

To quantify proliferating cells, we used a 5-bromo-2-deoxyuridine (BrdU) cell proliferation assay kit (Cell Signalling Technology, Euro Clone, Milan, Italy), according to the manufacturer's instructions.

Briefly, second passage primary podocytes were plated (5 replicates per each cell type) in 96-well plates (one plate was used per each time point) and left to adhere for 24 h. Then cell medium was replaced by medium containing 10 μM BrdU.

After 24 and 48 h, medium was removed and replaced by the fixing/denaturing solution provided by the kit, kept at room temperature for 30 min, and then removed. Cells were subsequently incubated with the primary mouse anti-BrdU antibody at room temperature for 1 h, followed by washing and application of the secondary HRP (horseradish peroxidase)-conjugated anti-mouse IgG. After washing, 3,3',5,5'-Tetramethylbenzidine (TMB) substrate was added to reveal peroxidase activity, followed by the "TMB Stop solution" included in the kit. Absorbance was read at 450 nm immediately after adding the Stop solution.

2.12. In vitro TrkB silencing

Cells were transfected with 200 pM siRNA duplexes using Lipofectamine2000 (Life Technologies, Monza, Italy) as transfection agent. We used a pool of 3 commercially available siRNAs complementary to TrkB mRNA. As control, non-targeting siRNAs were applied at the same concentration.

Transfection efficiency was determined by a fluorescent-tagged siRNA (Alexa-Fluor488; Amersham, PerkinElmer, Waltham, MA).

2.13. Statistical analyses

Data are presented as mean ± SD. At least three replicates were conducted for each in vitro experiment. Two-tail Student's t test was used for analysis of data when two

groups of data were compared. ANOVA test was applied when comparing more than 2 groups of data. P values <0.05 were considered significant.

2.14. Ethical approval

Animal protocols strictly adhered to the Public Health Service Policy on Humane Care and Use of Laboratory Animals (D.L.116-27/01/1992) and were approved by the Milan University Institutional Care and Ethical Treatment Committee (Prot.N. 07/13). All animals were housed on a 12-h light/dark cycle, and allowed free access to food and water. When appropriate, the animals were sacrificed by decapitation after anesthesia induced by intraperitoneal injection of 370 mg/Kg of Chloral hydrate.

3. Results

3.1. Co-culture assembly and validation of the albumin permeability assay

The selection of a membrane made of polyethylene terephthalate (PET), a material used in vascular grafts (Peck et al., 2012), was based on transparency and optimal resistance during processing for transmission electron microscopy (Fig 2A), which were not guaranteed by other membranes, such as those made of polycarbonate or polytetrafluoroethylene (PTFE) (Fig 2B).

Type IV collagen was utilized for coating both sides of the membrane, which ensured formation of endothelial monolayers (Fig 3A) and better preservation of the podocyte phenotype as indicated by more regular F-actin distribution and more evident Nephrin, synaptopodin positivity along elongated cell processes (Fig 3B), as compared to type I collagen.

To allow podocyte adhesion to the upper side of the membrane, endothelial cells, seeded on the lower side, had to be cultivated in presence of VEGF 5 ng/ml for one week (Fig 4A). In absence of VEGF, or in presence of lower concentrations, or with shorter VEGF treatment, podocytes did not attach to or detached from the membrane, when seeded as second or first population respectively (Fig 4B).

Transmission electron microscopy (TEM) was instrumental to evaluate cell health and observe intercellular contacts (Fig 5). Scanning electron microscopy (SEM) allowed assessment of the homogeneity of distribution of both cell types, particularly to confirm the absence of areas of the membrane not covered by cells (Fig 6).

An albumin permeability assay, performed by measuring passage of albumin from the lower endothelial compartment to the upper podocyte medium, was validated under different experimental conditions. As compared to the membrane alone, collagen coating reduced the passage of albumin, which increased progressively up to 2 hours and then reached a plateau (Fig 7A). Therefore, all subsequent measurements were conducted at the 2h time point.

Presence of either endothelial cells or podocytes reduced albumin permeability. Endothelial cells alone guaranteed for a better resistance to albumin passage through the filter than podocytes alone, and albumin was best retained when the three-layer was established (Fig 7B).

Afterwards, podocyte damage was induced by adding to the podocyte medium substances known to alter cell morphology and function, i.e. puromycin aminonucleoside (PAN, 10 µg/ml, 24h), and adriamycin (doxorubicin hydrochloride, 0.8 µM, 12h) (Fig 7C). Dose-dependent and time-dependent tests showed that the assay detected even minor changes (Fig 7D-E). For instance, increased passage of albumin was observed after only 2 hour application of 0.8 µM adriamycin.

Increased permeability was accompanied by structural cell changes, as shown by light and electron microscopy; podocytes showed severe damage with appearance of large cytoplasmic vacuoles and detachment from the membrane. Endothelial cells were less severely affected, but lost the monolayer distribution (Fig 7F-H).

3.2. Co-culture assembly with primary podocytes

In order to ascertain the possibility of using primary cells, the co-culture was assembled with primary podocytes from C57BL/6 and Balb/C mice. Presence of these cells did not result in changes of albumin permeability as compared to the cell line (Fig 8A).

Then, we utilized podocytes derived from animals spontaneously developing proteinuria, namely homozygous Rab3A-null mice (Giardino et al, 2009; Armelloni et al, 2012), raised in a C57BL/6 background, and homozygous Crv4 mice, which lack the metabotropic glutamate receptor 1 (Grm1) and have a Balb/C background (Puliti et al, 2011)

Presence of either Rab3A-KO or Crv4/Crv4 podocytes resulted in increased albumin permeability as compared to the 3D co-cultures assembled with primary podocytes obtained from wild type animals of corresponding background (Fig 8B). Increased permeability was not due to reduced cell number; on the contrary, Rab3A-null podocytes displayed higher proliferation rates than wild type cells (Fig 8C). There were no proliferation differences between Crv4/Crv4 and WT cells (Fig 8C).

3.3. Drug testing

To establish whether the 3D co-culture could be useful in drug testing, we used dexamethasone 100 μM and 10 μM (Guess et al., 2010) in order to apply the same concentrations reached in humans after intravenous injection and oral administration. Dexamethasone was added after 24h incubation with adriamycin, and led to

progressive reduction of albumin permeability, that was not observed with medium alone (Fig 9A).

Then, we used the same approach to evaluate the effects of Brain Derived Neurotrophic Factor (BDNF), a neurotrophin capable of treating proteinuria and glomerular lesions in zebrafish and mouse models of adriamycin nephropathy (Li et al., 2015). 200 ng/ml BDNF (human recombinant, QED Bioscience Inc., Histo Line, Milano, Italy) time-dependently decreased albumin permeability below control levels (Fig 9B). The action of BDNF was receptor-dependent, as confirmed by the blunted effect observed after silencing the BDNF receptor TrkB (Fig 9C). In parallel with reduction of albumin permeability, light and electron microscopy showed amelioration of cell morphology (Fig 9D, E).

3.4. Intercellular signaling

We have previously shown that podocytes contain synaptic-like vesicles undergoing spontaneous and regulated exocytosis with neurotransmitter release and express a variety of neurotransmitter receptors, including those for glutamate (Rastaldi et al., 2006).

Additionally, as it occurs at the blood brain barrier (Krizbai et al., 1998), the ionotropic glutamate receptor NMDAR and the metabotropic receptor Grm1 are present in human and mouse glomerular endothelial cells in vivo (Fig 10A, B). Immunofluorescence and western blot analysis confirmed expression of both receptors by the capillary endothelial cell line utilized to build our 3D co-culture (Fig 10C, D).

Addition for 30 min of 1mM glutamate (Sharp et al, 2003) to the endothelial side of the co-culture potently increased albumin permeability (Fig 11A), and the same effect was obtained by adding to the podocyte medium 5 nM alpha-latrotoxin (Fig 11A), a substance known to cause bulk synaptic exocytosis from neuronal cells (Südhof et

al., 2001) and induce glutamate release from podocytes (Rastaldi et al., 2006). In addition, both treatments caused increased endothelial p44/42-MAPK ($p = 0.008$) (Fig 11D).

Pre-incubation of endothelial cells with the NMDAR antagonist MK-801 was able to prevent albumin leakage from the filter and abolish 44/42-MAPK activation induced either by glutamate and by alpha-latrotoxin, whereas endothelial pre-incubation with the Grm1 antagonist CPCCOEt did not modify these values and application of both antagonists did not result in additive effects (Fig 11B-D).

3.5. Addition of a third cell population to the 3D co-culture

Being the co-culture suspended on a well-plate, a third cell population of cells can be grown at the bottom of the well.

As a first application, we utilized mesenchymal stem cells, which have been shown to contribute to glomerular repair by exerting immunomodulatory functions (Zoja et al., 2012).

To verify this possibility in our system, podocyte damage was induced by adriamycin incubation for 24h, then half of the co-culture inserts were moved to wells in which Hoechst-labeled cord blood-derived mesenchymal stem cells were previously seeded at the bottom. The other half was moved to wells containing standard medium only.

As compared to the inserts hung to wells containing standard medium, those positioned in presence of mesenchymal stem cells displayed time-dependent reduction of albumin permeability (Fig 12A). Staining for filamentous actin demonstrated the repairing effects of exposure to mesenchymal stem cells on both cell types (Fig 12C,D).

As expected, due to the pore size of the membrane, no labelled nuclei were present among podocytes at any time points. Additionally, no more than 1-2 Hoechst-positive nuclei were detected on the endothelial side, suggesting that the effect on albumin permeability was largely independent of cell migration (Fig 12B).

4. Discussion

The main advantage of the 3D co-culture model described here is that it is simpler to realize than other recently published methods (Slater et al., 2011; Bruggeman et al., 2012), therefore it can be largely adopted by the scientific community. Differently from what has been shown in the literature so far, we describe along with the methodology a number of applications ranging from drug testing to intercellular signaling studies, which can make our system a good complement to other research techniques.

Among distinctive features of this method, the use of collagen IV for membrane coating is relevant to preservation of podocyte properties and the formation of endothelial monolayers.

It is well known that the extracellular matrix, which includes basement membranes, regulates both tissue architecture and cell phenotype. Through matrix receptors, such as integrins, cells are able to sense matrix changes, which induce intracellular signals that regulate multiple cellular events, influencing survival, differentiation, and gene expression (Schwartz, 2001).

Type IV collagen is the physiological collagen present in the glomerular basement membrane to which both podocytes and endothelial cells adhere in vivo (Miner, 2011). Instead, collagen type I, which is largely utilized for growing podocytes in culture, appears in glomeruli during pathological conditions in both rodents and humans (Floege et al., 1992; Glick et al., 1992; Minto et al., 1993).

Of note, glomerular endothelial cells were found to form clumps when grown on collagen type I (Slater et al., 2011). Therefore, based on our data, it seems reasonable to recommend the use of collagen type IV not only for three-dimensional co-cultures, but also for two-dimensional cultures of single glomerular cell types.

Optimal adherence and growth of podocytes and endothelial cells on the two sides of the membrane was possible by seeding podocytes after one week exposure of the capillary endothelial cell line to VEGF.

The importance of VEGF for glomerular endothelial health is well established. VEGF-A is highly expressed by podocytes and sensed by endothelial cell receptors, playing an important role in glomerular development (Eremina and Quaggin, 2004). A number of research has proved that exquisite dosage sensitivity to VEGF-A exists in the developing glomerulus, as both reduced and increased expression of VEGF-A lead to profound changes in glomerular structure and function in mice (Eremina et al., 2007). The role of VEGF persists also in the mature glomerulus. Use of VEGF inhibitors is associated with damage to the glomerular endothelium in animal models and results in proteinuria in humans (Eremina et al., 2008), suggesting that local VEGF-A production is also required for maintenance of this specialized vascular bed.

In vitro studies have demonstrated that VEGF is required for full maturation of a human glomerular endothelial cell line (Satchell et al., 2006). Concordantly, our data confirm the role of VEGF in stimulating the capillary cells to acquire a phenotype more similar to a glomerular endothelium, which is essential to allow podocytes to remain adherent to the other side of the membrane. These data confirm that intercellular signaling between podocytes and endothelial cells is of key importance in vitro as well as in vivo, and potentially support the hypothesis that podocyte detachment, a common phenomenon observed in proteinuric diseases, might be related to altered messages received from the endothelial compartment (Haraldsson and Nyström, 2012).

By arranging the 3D system with podocytes on the upper side and endothelial cells on the lower side, we have been able to develop a reliable and sensitive albumin permeability assay in which passage of albumin from the lower to the upper compartment is driven by osmotic forces and is progressively halted by the

membrane itself, the collagen layers, and the presence of one or both cellular elements.

Interestingly, as it occurs in vivo, endothelial cells alone are able to retain more albumin than podocytes alone. The phenomenon was first documented during normal filtration by Ryan and Karnovsky, by detection of labeled albumin in glomeruli rapidly fixed in situ (Ryan and Karnovsky, 1976), and then confirmed along the years with the discovery that the positively charged endothelial glycocalix is the main responsible for albumin retention on the capillary side of the glomerular filter (Haraldsson et al., 2008).

The assay is sensitive enough to detect cell damage induced not only by toxic substances but also by genetic changes, as shown when the co-culture is assembled with primary podocytes obtained from mutant mice. Furthermore, the assay can be utilized to evaluate the ability of different drugs to restore filter permeability, and allows rapid dose-dependent and time-dependent drug testing which can help planning in vivo studies and limit the number of animal experiments. Importantly, when we detected permeability changes we could in parallel document structural cell modifications by microscopy and immunostaining.

In addition, the system facilitates studies on intercellular signaling, though an obvious limitation of this type of 3-D co-culture is the extreme simplification of the barrier, as represented by the absence of proper slit diaphragms among podocyte cell processes as well as by the absence of the hemodynamic component.

Our experiments, by showing that excessive glutamate is harmful to endothelial cells, seem to support a series of analogies between the glomerular filtration barrier and the blood brain barrier; endothelial permeability increases in response to excessive glutamate, and is due to abnormal activation of the NMDA glutamate receptor (Sharp et al., 2003). Increased glutamate in the circulation can be found in a variety of conditions, the most common being fever, in which is not infrequent to observe mild

and reversible albuminuria (Lillehoj and Poulik, 1986). In addition, increased glutamate at the filtration barrier can derive from altered podocyte signaling (Armelloni et al., 2012). As shown by the experiments conducted with alpha-latrotoxin, these changes have similar consequences on permeability and use similar activation pathways as the direct addition of glutamate to endothelial cells.

We have finally exploited the possibility of adding a third cell population to the co-culture utilizing mesenchymal stem cells grown at the bottom of the well, which confirmed the beneficial effect of this cell type on podocyte damage previously observed in vivo (Zoja et al., 2012).

We have recently described the treatment with human allogeneic bone marrow mesenchymal stem cells in a pediatric patient developing recurrent focal segmental glomerulosclerosis (FSGS) after renal transplantation and not responding to conventional therapy (Belingheri et al., 2013). Furthermore, a human trial has been recently approved at the Policlinic of Milano for treating non-responding FSGS patients with CBMSCs. In this respect, besides standard immunological assays which are performed to select the best available CBMSCs preparations to be infused in the single patient, an additional permeability test on the 3D co-culture might further help the selection process.

5. Conclusions

In summary, our results seem to show that a 3D co-culture of podocytes and endothelial cells is not only feasible, but can be utilized in a number of applications ranging from drug testing to studies of intercellular signaling, and can complement successfully numerous in vitro and in vivo research methodologies to investigate the complex function of the glomerular filtration barrier.

Acknowledgements

The work was supported by funding from Associazione Bambino Nefropatico ABN ONLUS, Milano, Italy. The Renal Research Laboratory and the Cell Factory of Milan Policlinic and the Laboratory of Renal Physiopathology of Trieste University belong to the "Italian Network to fight FSGS" organized and supported by "Fondazione la Nuova Speranza ONLUS - Lotta alla Glomerulosclerosi Focale", Rho (Mi).

References

Armelloni S, Calvaresi N, Ikehata M, Corbelli A, Mattinzoli D, Giardino LA, et al., 2012. Proteinuria and glomerular damage in Rab3A knockout mice chronically fed a high-glucose diet. Nephron Exp Nephrol. 120:e69-80.

Armelloni S, Li M, Messa P, Rastaldi MP., 2012. Podocytes: a new player for glutamate signaling. Int J Biochem Cell Biol. 44:2272-7.

Avner ED, Sweeney WE Jr., 1990. Polypeptide growth factors in metanephric growth and segmental nephrin differentiation. Pediatr Nephrol. 4:372-7.

Avner ED, Villee DB, Schneeberger EE, Grupe WE., 1983. An organ culture model for the study of metanephric development. J Urol 129:660-4.

Barilani M, Lavazza C, Viganò M, Montemurro T, Boldrin V, Parazzi V, et al., 2015. Dissection of the cord blood stromal component reveals predictive parameters for culture outcome. Stem Cells Dev. 24:104-14.

Belingheri M, Lazzari L, Parazzi V, Groppali E, Biagi E, Gaipa G, et al., 2013. Allogeneic mesenchymal stem cell infusion for the stabilization of focal segmental glomerulosclerosis. Biologicals. 41:439-45.

Bruggeman LA, Doan RP, Loftis J, Darr A, Calabro A., 2012. A cell culture system for the structure and hydrogel properties of basement membranes; Application to capillary walls. Cell Mol Bioeng 5:194-204.

Chen J, Braet F, Brodsky S, Weinstein T, Romanov V, Noiri E, et al., 2002. VEGF-induced mobilization of caveolae and increase in permeability of endothelial cells. Am J Physiol Cell Physiol. 282:C1053-63.

Eremina V, Baelde HJ, Quaggin SE., 2007. Role of the VEGF--a signaling pathway in the glomerulus: evidence for crosstalk between components of the glomerular filtration barrier. Nephron Physiol. 106:p32-7.

Eremina V, Jefferson JA, Kowalewska J, Hochster H, Haas M, Weisstuch J, et al., 2008. VEGF inhibition and renal thrombotic microangiopathy. N Engl J Med. 358:1129-36.

Eremina V, Quaggin SE., 2004. The role of VEGF-A in glomerular development and function. Curr Opin Nephrol Hypertens. 13:9-15.

Floege J, Johnson RJ, Gordon K, Yoshimura A, Campbell C, Iruela-Arispe L, et al., 1992. Altered glomerular extracellular matrix synthesis in experimental membranous nephropathy. Kidney Int. 42:573-85.

Garg P, Rabelink T., 2011. Glomerular proteinuria: a complex interplay between unique players. Adv Chronic Kidney Dis. 18:233-42.

Giardino L, Armelloni S, Corbelli A, Mattinzoli D, Zennaro C, Guerrot D, et al., 2009. Podocyte glutamatergic signaling contributes to the function of the glomerular filtration barrier. J Am Soc Nephrol. 20:1929-40.

Glick AD, Jacobson HR, Haralson MA., 1992. Mesangial deposition of type I collagen in human glomerulosclerosis. Hum Pathol. 23:1373-9.

Guess A, Agrawal S, Wei CC, Ransom RF, Benndorf R, Smoyer WE., 2010. Dose- and time-dependent glucocorticoid receptor signaling in podocytes. Am J Physiol Renal Physiol. 299:F845-53.

Haraldsson B, Nystrom J, Deen WM., 2008. Properties of the glomerular barrier and mechanisms of proteinuria. Physiol Rev 88:451–87.

Haraldsson B, Nyström J., 2012. The glomerular endothelium: new insights on function and structure. Curr Opin Nephrol Hypertens. 21:258-63.

Hirschberg R, Wang S, Mitu GM., 2008. Functional symbiosis between endothelium and epithelial cells in glomeruli. Cell Tissue Res. 331:485-93.

Kim BS, Chen J, Weinstein T, Noiri E, Goligorsky MS., 2002. VEGF expression in hypoxia and hyperglycemia: reciprocal effect on branching angiogenesis in epithelial-endothelial co-cultures. J Am Soc Nephrol. 13:2027-36.

Kloth S, Aigner J, Kubitza M, Schmidbauer A, Gerdes J, Moll R, et al., 1995. Development of renal podocytes cultured under medium perifusion. Lab Invest 73:294-301.

Krizbai IA, Deli MA, Pestenácz A, Siklós L, Szabó CA, András I, et al., 1998. Expression of glutamate receptors on cultured cerebral endothelial cells. J Neurosci Res. 54:814-9.

Li M, Armelloni S, Zennaro C, Wei C, Corbelli A, Ikehata M, et al., 2015. BDNF repairs podocyte damage by microRNA-mediated increase of actin polymerization. J Pathol. 235:731-44.

Lillehoj EP, Poulik MD., 1986. Normal and abnormal aspects of proteinuria. Part I: Mechanisms, characteristics and analyses of urinary protein. Part II: Clinical considerations. Exp Pathol. 29:1-28.

Miner JH., 2011. Glomerular basement membrane composition and the filtration barrier. Pediatr Nephrol. 26:1413-7.

Minto AW, Fogel MA, Natori Y, O'Meara YM, Abrahamson DR, Smith B, et al., 1993. Expression of type I collagen mRNA in glomeruli of rats with passive Heymann nephritis. Kidney Int. 43:121-7.

Mundel P, Reiser J, Zuniga Mejıa Borja A, Pavenstaedt H, Davidson GR, Kriz W. et al., 1997. Rearrangements of the cytoskeleton and cell contacts induce process

formation during differentiation of conditionally immortalized mouse podocyte cell lines. Exp Cell Res 236:248–58.

Obeidat M, Ballermann BJ., 2012. Glomerular endothelium: a porous sieve and formidable barrier. Exp Cell Res. 318:964-72.

Obeso J, Weber J, Auerbach R., 1990. A hemangioendothelioma-derived cell line: its use as a model for the study of endothelial cell biology. Lab Invest. 63:259-69.

Peck M, Gebhart D, Dusserre N, McAllister TN, L'Heureux N., 2012. The evolution of vascular tissue engineering and current state of the art. Cells Tissues Organs. 195:144-58.

Puliti A, Rossi PI, Caridi G, Corbelli A, Ikehata M, Armelloni S, et al., 2011. Albuminuria and glomerular damage in mice lacking the metabotropic glutamate receptor 1. Am J Pathol. 178:1257-69.

Rastaldi MP, Armelloni S, Berra S, Calvaresi N, Corbelli A, Giardino LA, et al., 2006. Glomerular podocytes contain neuron-like functional synaptic vesicles. FASEB J. 20:976-8.

Reiser J, Sever S., 2013. Podocyte biology and pathogenesis of kidney disease. Annu Rev Med. 64:357-66.

Ryan GB, Karnovsky MJ., 1976. Distribution of endogenous albumin in the rat glomerulus: role of hemodynamic factors in glomerular barrier function. Kidney Int 9:36–45.

Satchell SC, Tasman CH, Singh A, Ni L, Geelen J, von Ruhland CJ, et al., 2006. Conditionally immortalized human glomerular endothelial cells expressing fenestrations in response to VEGF. Kidney Int. 69:1633-40.

Schwartz MA., 2001. Integrin signaling revisited. Trends Cell Biol. 11:466-70.

Sharp CD, Hines I, Houghton J, Warren A, Jackson TH 4th, Jawahar A, et al., 2003. Glutamate causes a loss in human cerebral endothelial barrier integrity through activation of NMDA receptor. Am J Physiol Heart Circ Physiol. 285:H2592-8.

Sharp CD, Hines I, Houghton J, Warren A, Jackson TH 4th, Jawahar A, et al., 2003. Glutamate causes a loss in human cerebral endothelial barrier integrity through activation of NMDA receptor. Am J Physiol Heart Circ Physiol. 285:H2592-8.

Slater SC, Beachley V, Hayes T, Zhang D, Welsh GI, Saleem MA, et al., 2011. An in vitro model of the glomerular capillary wall using electrospun collagen nanofibres in a bioartificial composite basement membrane. PLoS One. 6(6):e20802.

Südhof TC., 2001. alpha-Latrotoxin and its receptors: neurexins and CIRL/latrophilins. Annu Rev Neurosci. 24:933-62.

Zoja C, Garcia PB, Rota C, Conti S, Gagliardini E, Corna D, et al., 2012. Mesenchymal stem cell therapy promotes renal repair by limiting glomerular podocyte and progenitor cell dysfunction in adriamycin-induced nephropathy. Am J Physiol Renal Physiol. 303:F1370-81.

Legends to Figures

Fig 1. Characterization of the endothelial cell line by immunofluorescence microscopy. The selected capillary cell line shows expression of CD31, VE-cadherin, and vWF (in green). Furthermore, uptake of acetylated-LDL can be observed after incubation of the cell line with acetylated LDL labelled by DiI (in red). Scale bars: CD31, VE-cadherin, vWF: 100 µm, DiI-acetylated-LDL: 200 µm.

Figure 2. Appearance of different membranes after processing for transmission electron microscopy (TEM). Representative TEM images of a membrane made of polyethylene terephthalate (PET) (A) and a membrane made of polytetrafluoroethylene (PTFE) (B), both covered on one side by a cell layer. The PET membrane is compact and unaltered, whereas PTFE did not resist to processing, as shown by the formation of numerous holes in its structure. Scale bars: 5 µm.

Figure 3. Effects of collagen types on endothelial cells and podocytes. (A) A uniform monolayer of endothelial cells, stained by the endothelial cell marker CD31, is obtained in presence of collagen type IV (upper panel), whereas only small groups of cells can be observed when coating is performed with collagen type I (lower panel). (B) In presence of collagen type IV (left panels) podocytes show actin stress fibers (stained by Phalloidin–TRITC), nephrin can be detected along cell processes, and synaptopodin is observed in the cell body and along cell processes. After collagen type I coating (right panels), podocytes display mainly cortical actin, nephrin is no longer detectable along cell processes, and synaptopodin staining is decreased. Scale bars: A): 200 µm; B): 100 µm.

Figure 4. Effects of VEGF on the co-culture assembly. (A) Both endothelial cells (blue arrow) and podocytes (red arrow) adhere to the opposite sides of the membrane after endothelial cell incubation with VEGF. (B) Only endothelial cells

remain attached to the membrane when VEGF has been omitted from the endothelial cell medium. Scale bars: A): 40 µm; B): 80 µm.

Figure 5. Cell morphology by TEM. TEM images from (A) endothelial cells and (B) podocytes reveal the presence of healthy cells on both sides of a membrane. Neighboring endothelial cells make multiple cell contacts, and podocytes reach each other through cell processes (red arrows). Scale bars: A): 500 nm; B): 1 µm.

Figure 6. Scanning electron microscopy (SEM). Observation by SEM demonstrates the homogeneous monolayer distribution of both endothelial cells (A) and podocytes (B), and shows that the membrane is completely covered by cells on both sides. Scale bars: 20 µm.

Figure 7. Albumin permeability assay. (A) Albumin passage through the membrane not covered by cells was assessed without (black line) and with (grey line) collagen coating. In both conditions, albumin is retrieved in the upper medium in progressively higher concentration from 30 to 120 minutes. Then, albumin concentration remains almost identical. Presence of coating lowers albumin concentration at any time points and ensures a more regular progression with time. (B) At the time point of 120 minutes, concentration of albumin in the upper compartment is progressively reduced by the presence of one cell population. Endothelial cells more efficiently than podocytes reduce albumin passage through the membrane. The highest resistance to albumin passage is obtained in presence of both cell types. (C) Damage to podocytes by addition to the podocyte medium of puromycin aminonucleoside (PAN, 10 µg/ml, 24h), or adriamycin (doxorubicin hydrochloride, 0.8 µM, 12h) increases albumin concentration in the podocyte medium. (D) Adriamycin has a dose-dependent effect on albumin permeability which becomes significant at the dose of 0.5 µM. (E) 0.8 µM adriamycin has a time-dependent effect on albumin permeability, which becomes significant after 6 hours. (F) The morphological effects of adriamycin can be observed by light microscopy: the

upper side of the membrane appears devoid of cells and the lower side shows the presence of more than one cell layers. (G) TEM displays podocyte damage after adriamycin incubation, with numerous cytoplasmic vacuoles. (H) TEM observation of the lower side of the membrane after adriamycin incubation shows the formation of multiple layers of endothelial cells. *p<0.05; **p<0.01. Scale bars: F): 40 μm; G) and H): 1 μm.

Figure 8. Co-culture assembly with primary podocytes. (A) Presence of primary podocytes on the upper side of the membrane does not modify albumin permeability, as compared to the cell line. (B) Presence of podocytes from both Rab3A-KO mice and homozygous crv4 mutants results in significantly higher concentration of albumin in the podocyte medium, as compared to the primary cells obtained from wild type animals. (C) Cell proliferation is significantly higher in Rab3A-KO-derived podocytes than in the other primary cells. *p<0.05; **p<0.01.

Figure 9. Drug testing experiments. (A) After adriamycin-induced podocyte damage, dexamethasone reduces albumin permeability. Efficacy of treatment with dexamethasone 100 μM is already evident at 24h, whereas 48h are needed to reduce permeability with dexamethasone 10 μM. At 72 hours both dosages show the same effect. (B) After podocyte incubation with adriamycin, BDNF time-dependently decreases albumin permeability. (C) BDNF effects on albumin permeability are confirmed in cells transfected with non-targeting siRNAs (black bars), but are reduced in cells transfected with a pool of siRNAs complementary to the mRNA of the BDNF receptor TrkB. (D) Light microscopy (left panel) shows detachment of podocytes and formation of multiple layers of endothelial cells after adriamycin treatment. TEM confirms podocyte damage with detachment from the membrane and presence of multiple cytoplasmic vacuoles (middle panel), and multi-layering of endothelial cells (right panel). (E) After BDNF treatment, light microscopy shows covering of both sides of the membrane by uniform monolayers of cells (left panel).

TEM illustrates that both podocytes (middle panel) and endothelial cells (right panel) look healthy. *p<0.05; **p<0.01. Scale bars: D): 20 μm, 300 nm, 2 μm; E) 20 μm, 500nm, 1 μm.

Figure 10. Glutamate receptor expression by endothelial cells. (A) The ionotropic glutamate receptor NMDAR1 (in red) partially co-localizes (yellow spots) with the endothelial marker CD31 (in green) in a glomerulus from a mouse control kidney. (B) Expression of NMDAR1 (left panel) and metabotropic glutamate receptor 1 (Grm1) (right panel) on glomerular endothelium (red arrows) can be visualized by immunogold electron microscopy in mouse renal glomeruli. Additional gold particles (blue arrows) are present on podocytes. (C) Immunostaining and (D) western blot show that NMDAR1 and Grm1 are expressed by the endothelial cell line utilized in the 3D co-culture. WB: protein extracts from 2 preparations of the endothelial cell line were loaded on lanes 1-4. Buffer was loaded on lane 5 as negative control. Upper panels show NMDAR1 (lanes 1, 2) and Grm1 (lanes 3, 4, 5). VE-cadherin, used as loading control, is shown in the lower panels (lanes 1-5). MWM: molecular weight marker. Scale bars: A): 20 μm; B) 300 nm; C): 100 μm.

Figure 11. Glutamate toxicity on endothelial cells. (A) Significant increase in albumin permeability is observed after addition of glutamate to the endothelial cell medium or after podocyte incubation with alpha-latrotoxin (LTX). (B, C) Pre-incubation of endothelial cells with the NMDAR antagonist MK-801, but not with the Grm1 antagonist CPCCOEt, prevents the increase in albumin permeability due to addition of glutamate to endothelial cells (B) or to LTX addition to the podocyte medium (C). In both cases, pre-incubation of endothelial cells with both glutamate receptor antagonists does not result in additive effects. (D) Both glutamate and LTX activated increased 44/42MAPK activation as expressed by increased ratio between total and phosphorylated MAPK examined by in-cell ELISA. Pre-incubation of

endothelial cells with MK-801, but not with CPCCOEt, abolished MAPK activation and application of both antagonists did not have additive effects. *p<0.05; **p<0.01.

Figure 12. Effects of mesenchymal stem cells on filter permeability. (A) After adriamycin incubation, albumin permeability time-dependently increases in inserts exposed to medium only. In presence of mesenchymal stem cells permeability time-dependently significantly diminishes. (B) One Hoescht-labelled blue nucleus can be observed at the endothelial side after 48 incubation of the insert in presence of mesenchymal stem cells. (C) Staining of filamentous actin (F-actin) by phalloidin-TRITC allows observation of small groups of endothelial cells (left panel) and a non-homogeneous layer of podocytes (right panel) with mostly cortical actin, after adriamycin incubation and exposure of the insert to medium alone for 48h. (D) In presence of mesenchymal stem cells, F-actin staining shows a better distribution of both endothelial cells (left panel) and podocytes (right panel) along the respective sides of the membrane and the reappearance of stress fibers in podocytes. **p<0.01. Scale bars B), C), D): 200 µm.

Figure(s)
Click here to download high resolution image

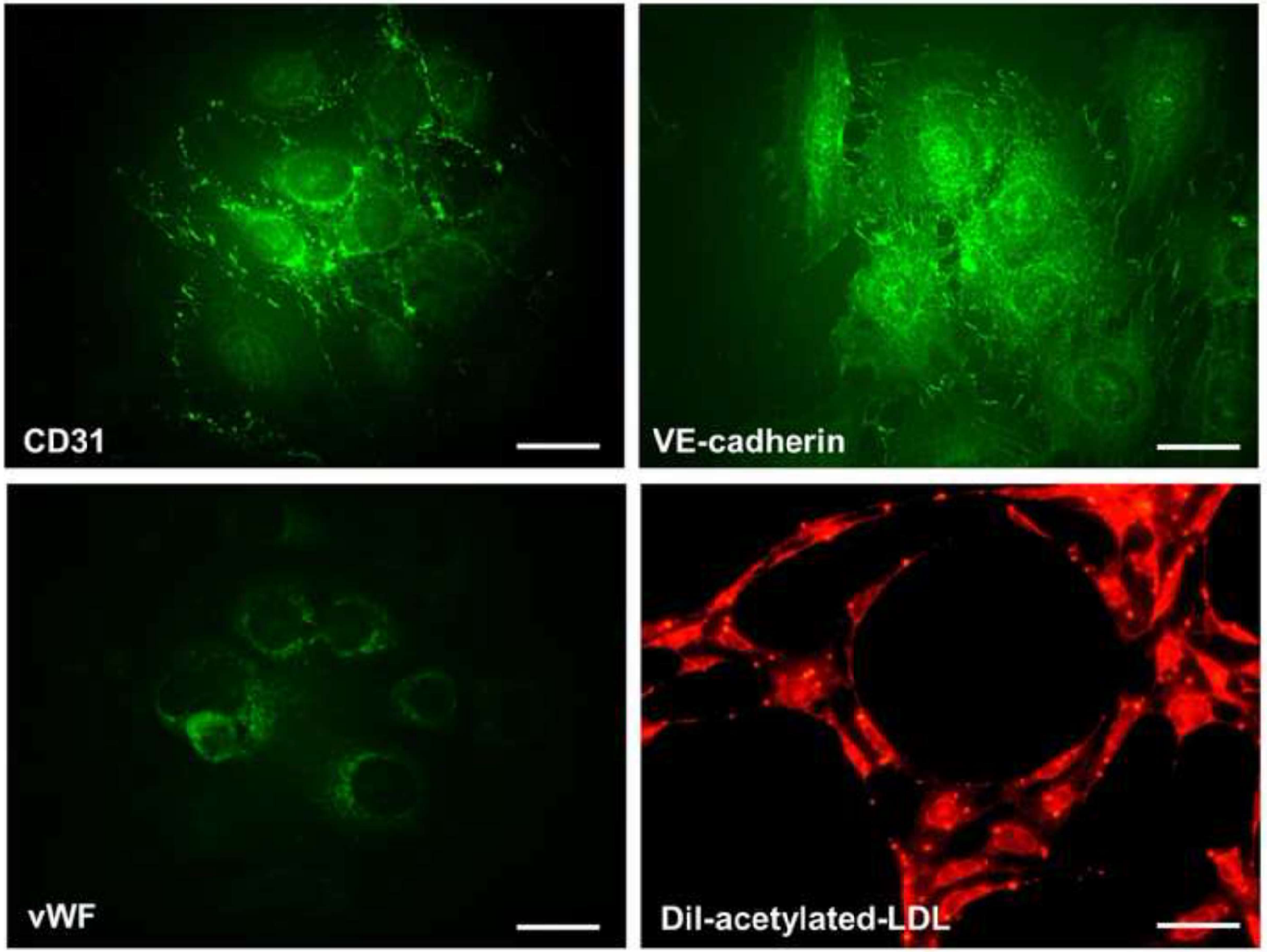

Figure(s)
Click here to download high resolution image

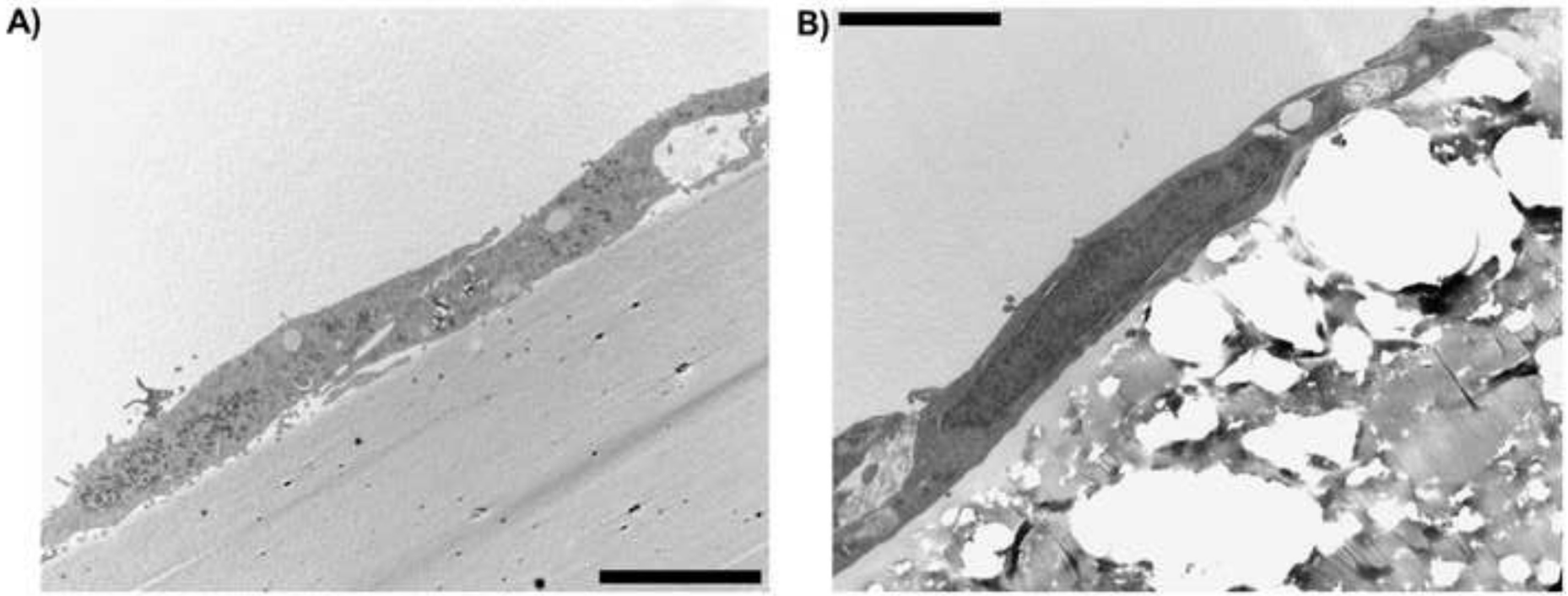

Figure(s)
Click here to download high resolution image

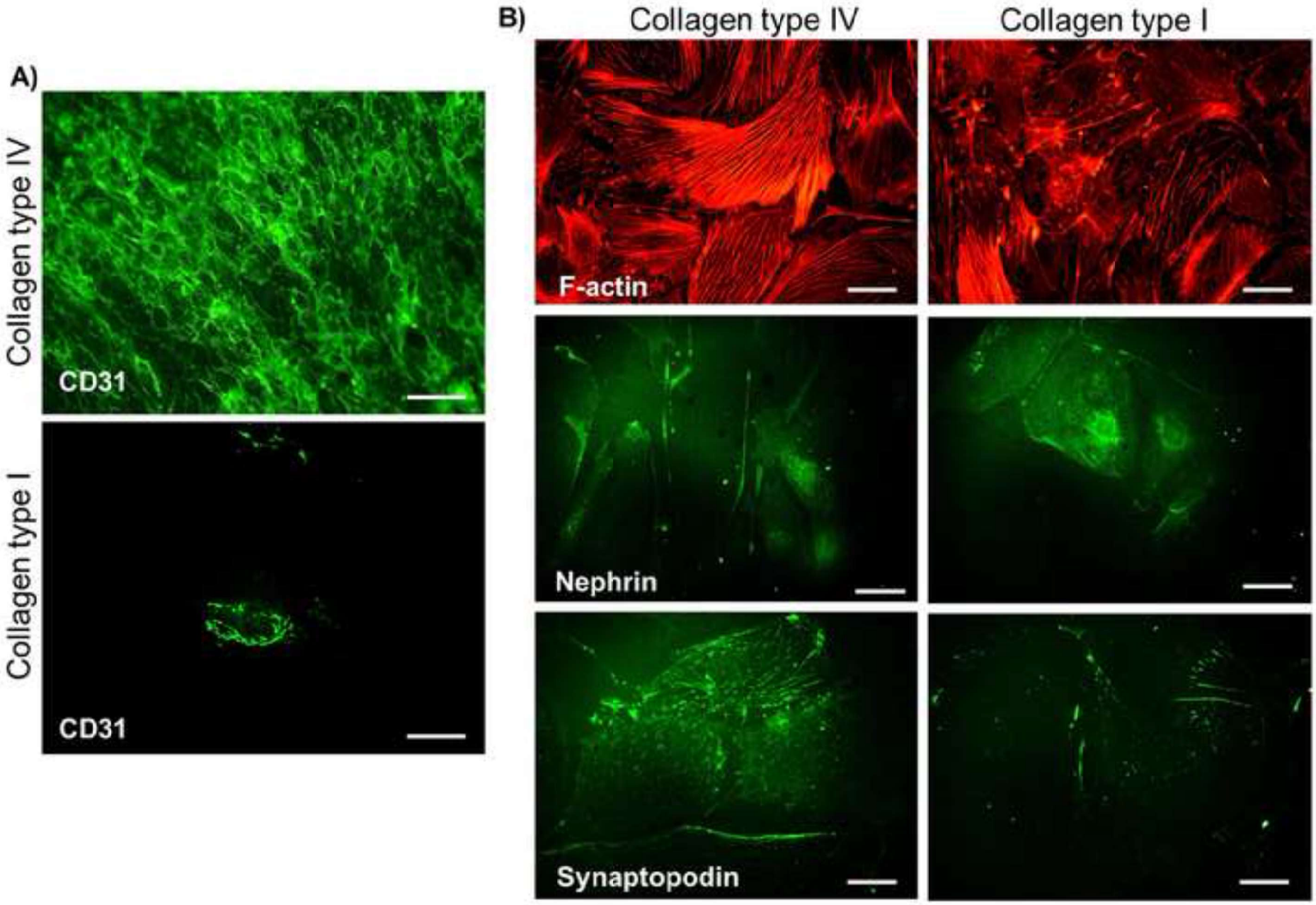

Figure(s)
Click here to download high resolution image

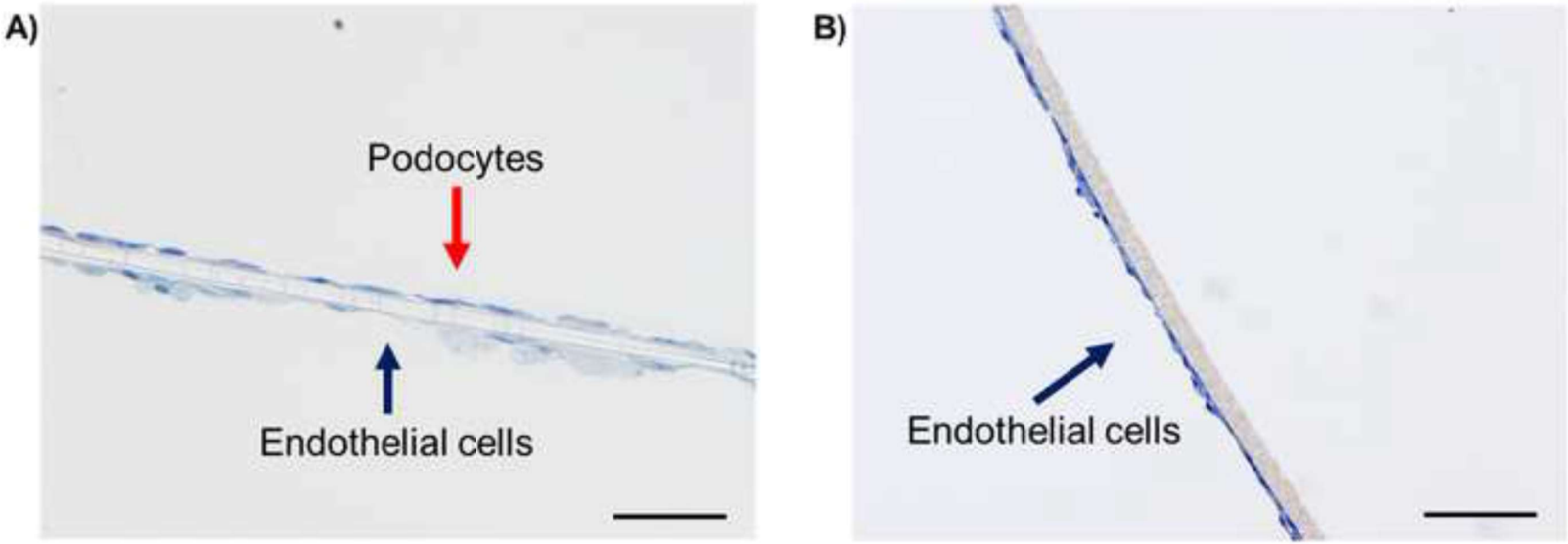

Figure(s)

Click here to download high resolution image

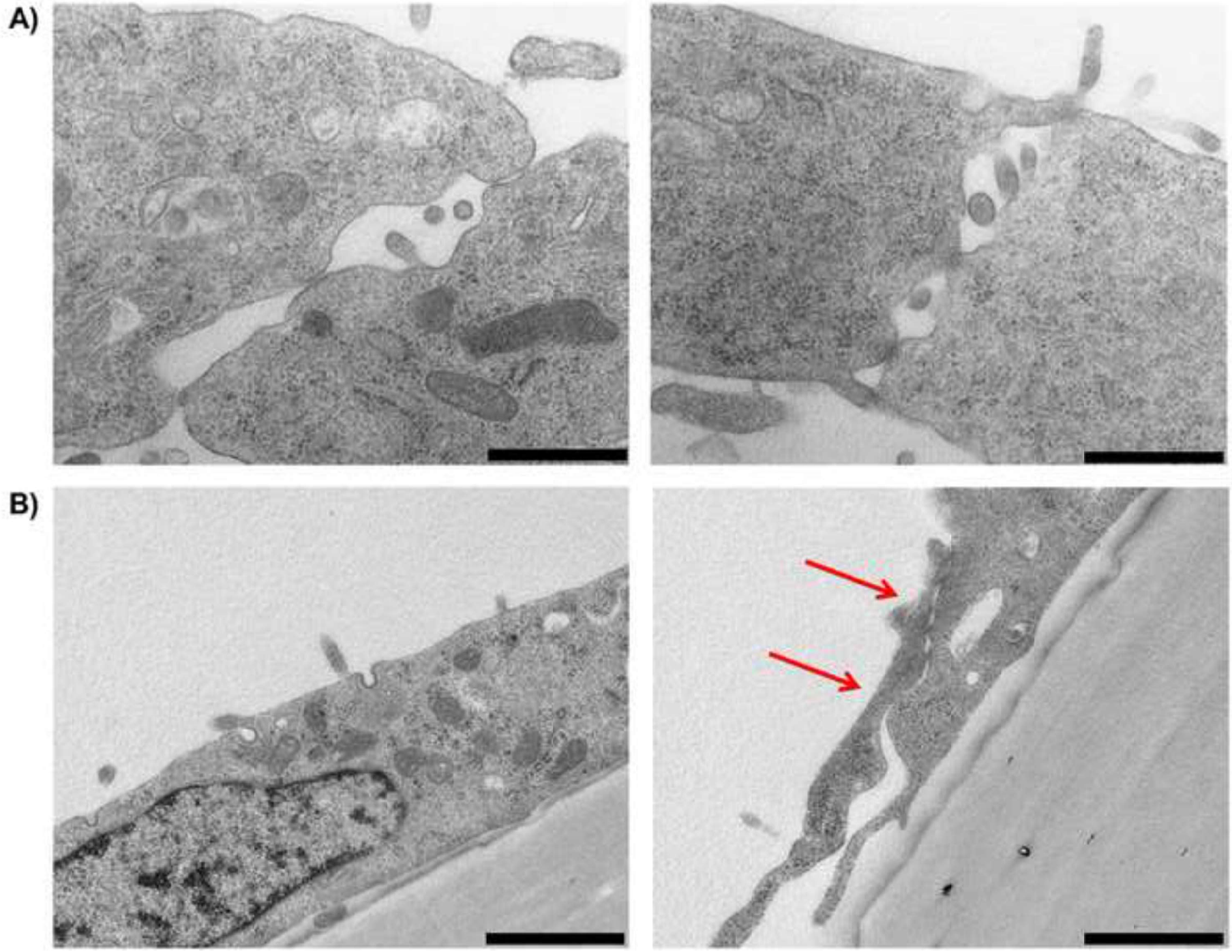

Figure(s)
Click here to download high resolution image

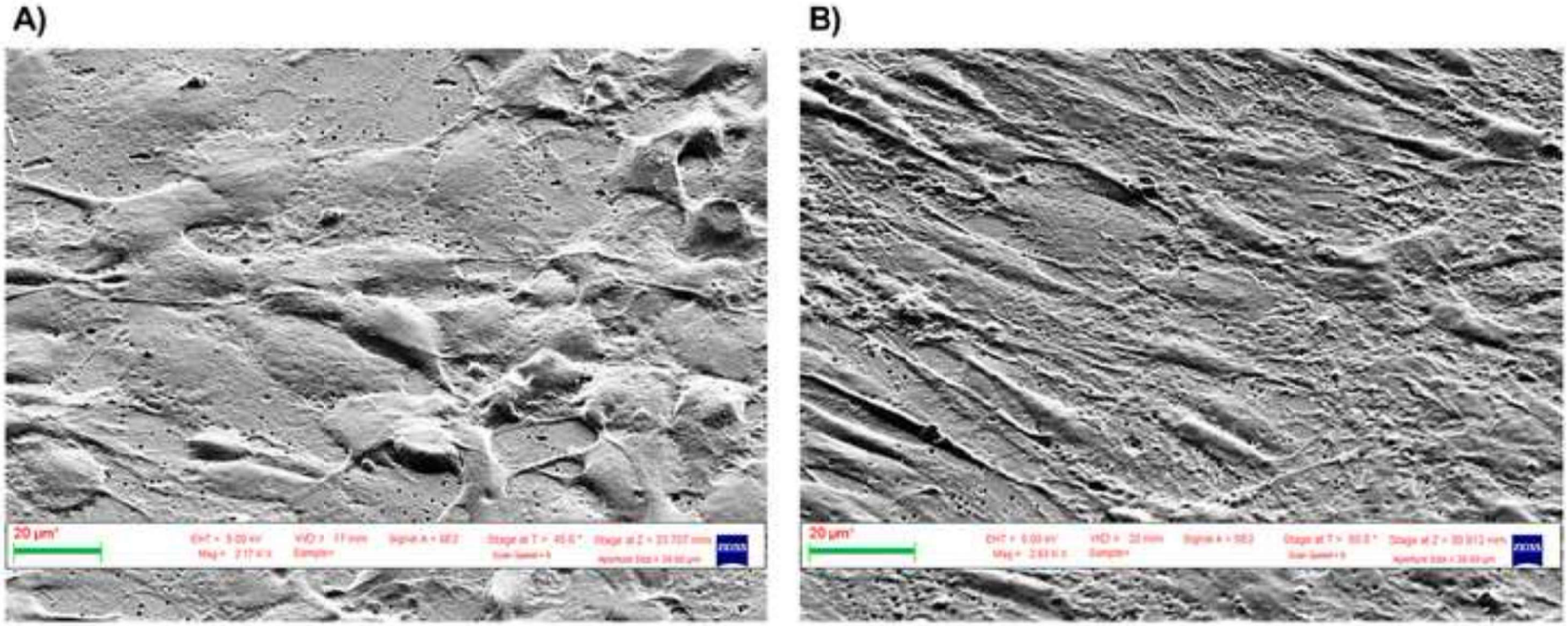

Figure(s)
Click here to download high resolution image

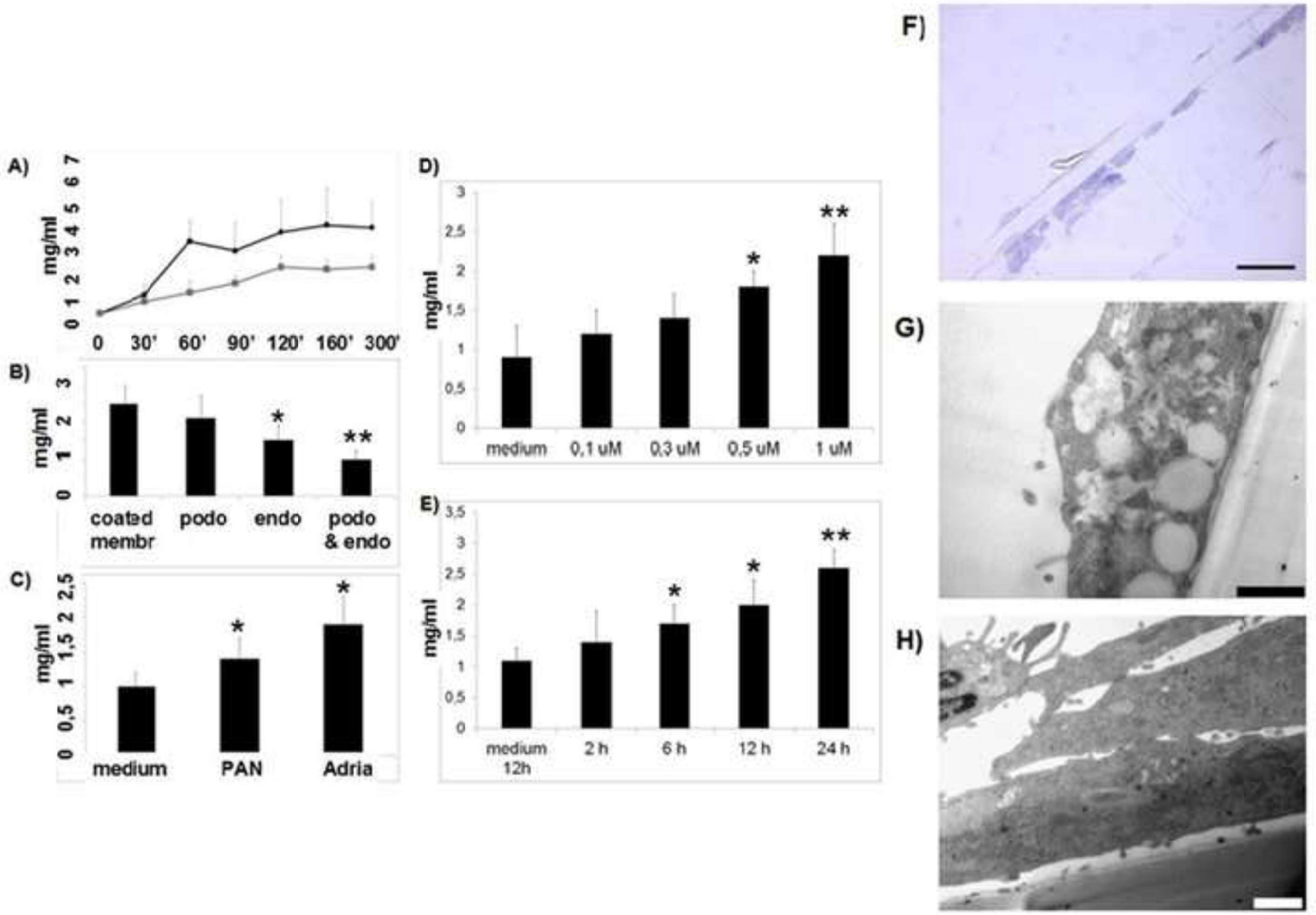

Figure(s)

Click here to download high resolution image

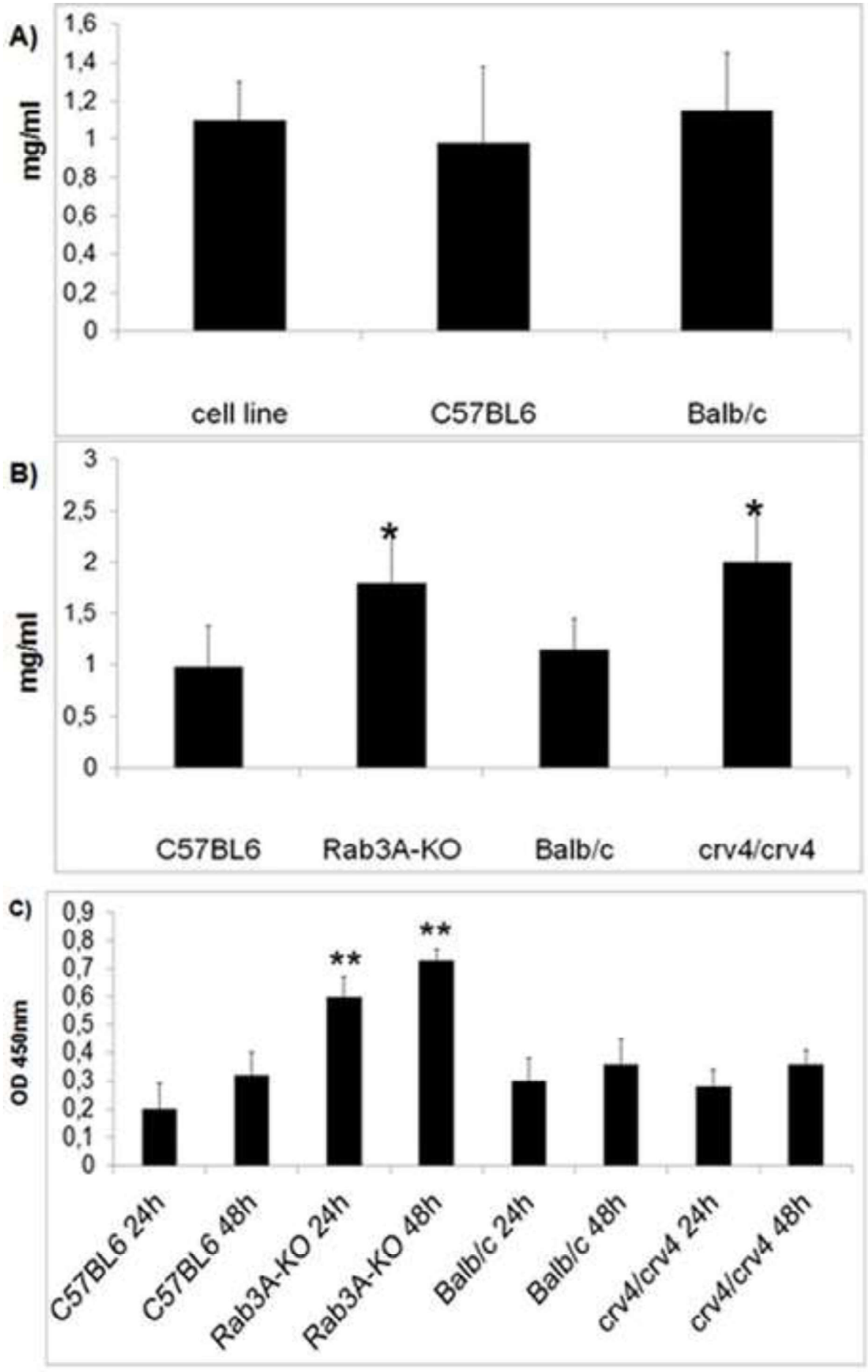

Figure(s)

Click here to download high resolution image

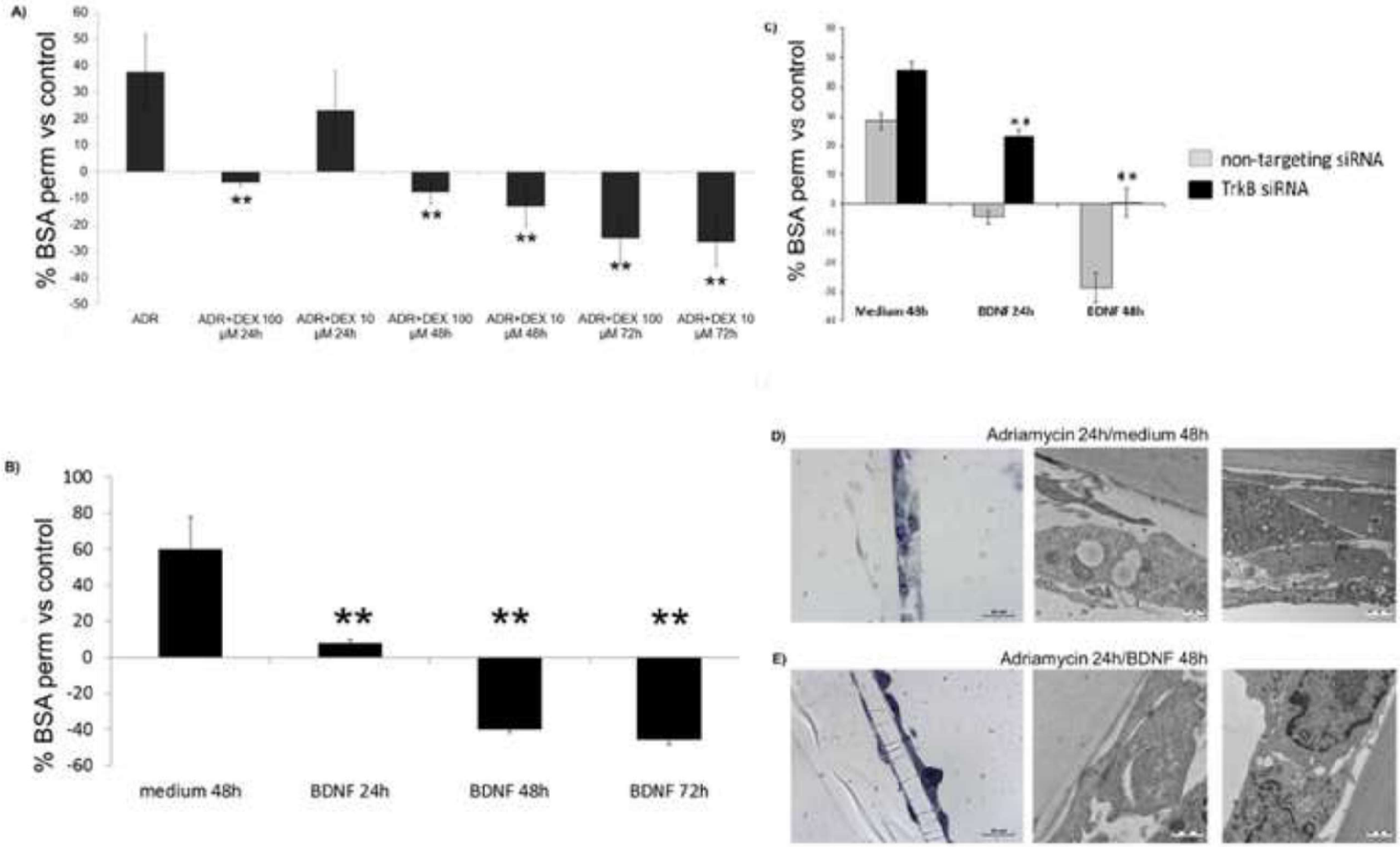

Figure(s)
Click here to download high resolution image

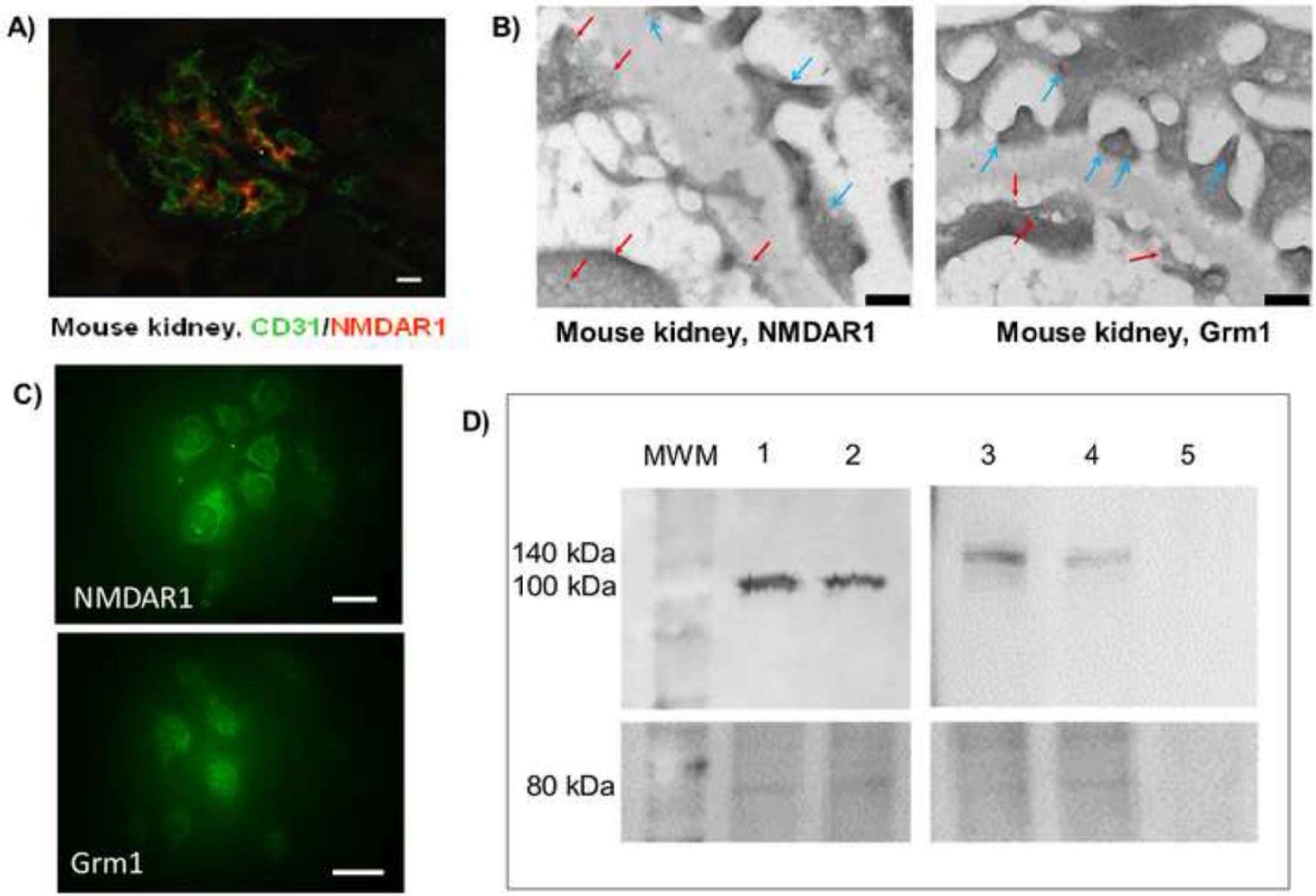

Figure(s)
Click here to download high resolution image

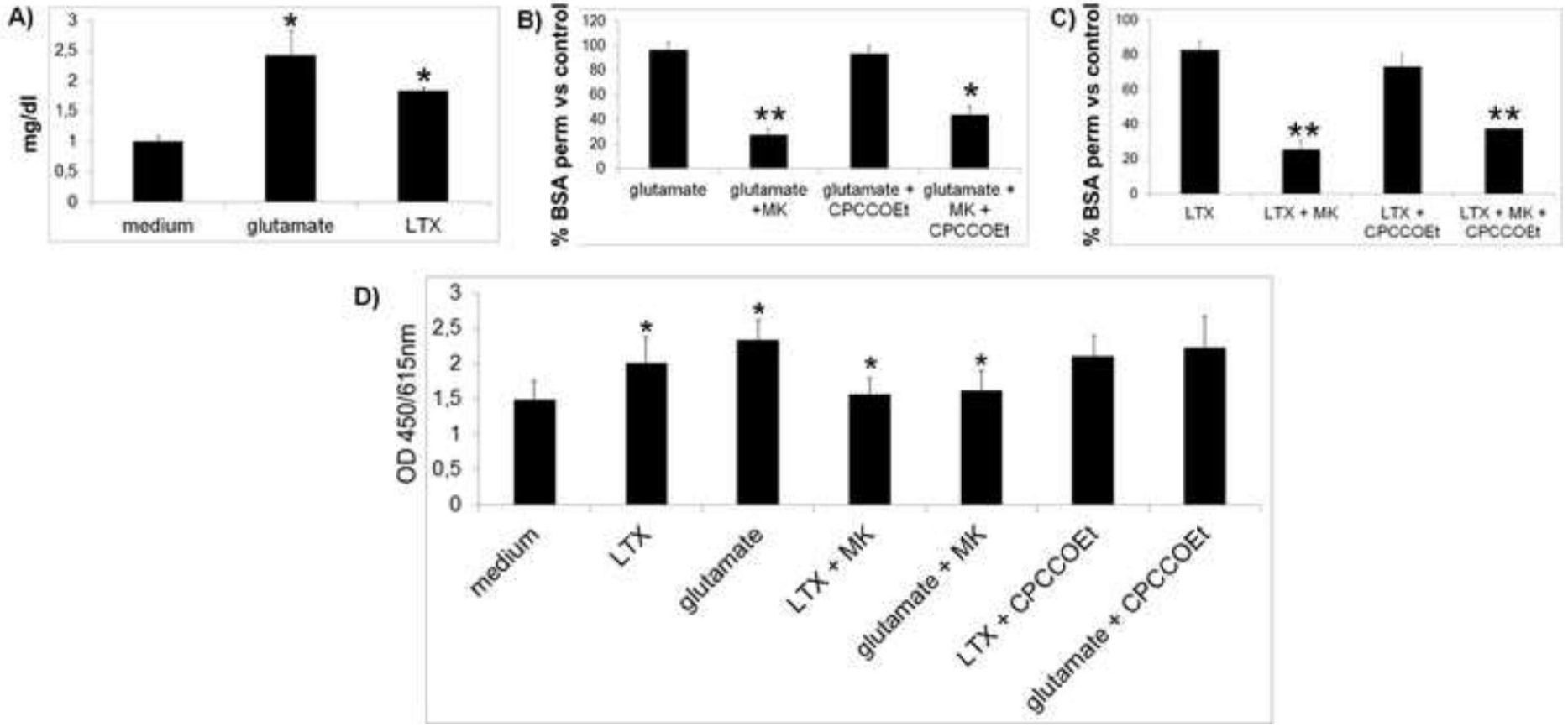

Figure(s)
Click here to download high resolution image